Chapter 1

Finite Elements Overview

1.1 Modeling Basics

"There are no exact answers. Just bad ones, good ones and better ones. Engineering is the art of approximation." Approximation is performed with models. We consider a reality of interest, e.g., a concrete beam. In a first view, it has *properties* such as dimensions, color, surface texture. From a view of structural analysis the latter ones are irrelevant. A more detailed inspection reveals a lot of more properties: composition, weight, strength, stiffness, temperatures, conductivities, capacities, and so on. From a structural point of view some of them are essential. We combine those essential properties to form a *conceptual model*. Whether a property is essential is obvious for some, but the valuation of others might be doubtful. We have to choose. By choosing properties our model becomes approximate compared to reality. Approximations are more or less accurate.

On one hand, we should reduce the number of properties of a model. Any reduction of properties will make a model less accurate. Nevertheless, it might remain a good model. On the other hand, an over-reduction of properties will make a model inaccurate and therefore useless. Maybe also properties are introduced which have no counterparts in the reality of interest. Conceptual modeling is the art of choosing properties. As all other arts it cannot be performed guided by strict rules.

The chosen properties have to be related to each other in quantitative manner. This leads to a *mathematical model*. In many cases, we have systems of differential equations relating variable properties or simply *variables*. After prescribing appropriate boundary and initial conditions an exact, unique solution should exist for variables depending on spatial coordinates and time. Thus, a particular variable forms a field. Such fields of variables are infinite as space and time are infinite.

As analytical solutions are not available in many cases, a discretization is performed to obtain approximate numerical solutions. *Discretization* reduces underlying infinite space and time into a finite number of supporting points in space and time and maps differential equations into algebraic equations relating a finite number of variables. This leads to a *numerical model*.

Computational Methods for Reinforced Concrete Structures. First Edition. Ulrich Häussler-Combe.

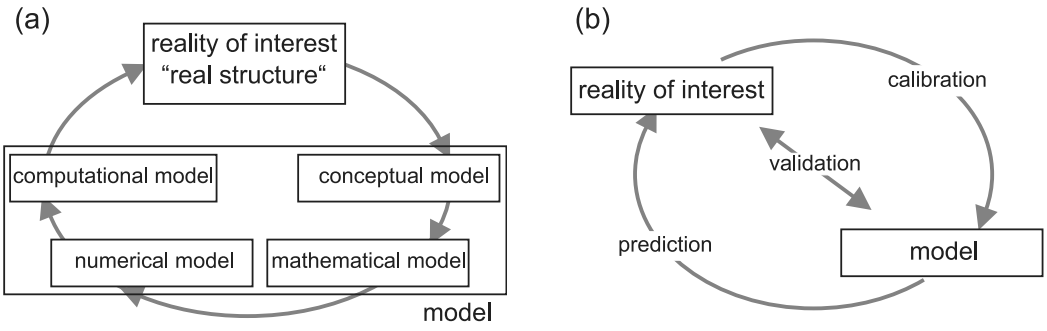

Figure 1.1: Modeling (a) Type of models following [83]. (b) Relations between model and reality.

A numerical model needs some completion as it has to be described by means of programming to form a *computational model*. Finally, programs yield solutions through processing by computers. The whole cycle is shown in Fig. 1.1. Sometimes it is appropriate to merge the sophisticated sequence of models into the *model*.

A final solution provided after computer processing is approximate compared to the exact solution of the underlying mathematical model. This is caused by discretization and round-off errors. Let us assume that we can minimize this mathematical approximation error in some sense and consider the final solution as a *model solution*. Nevertheless, the relation between the model solution and the underlying reality of interest is basically an issue. Both – model and reality of interest – share the same properties by definition or conceptual modeling, respectively. Let us also assume that the real data of properties can be objectively determined, e.g., by measurements.

Thus, real data of properties should be properly approximated by their computed model counterparts for a problem under consideration. The difference between model solution data and real data yields a *modeling error*. In order to distinguish between bad (inaccurate), good (accurate), and better model solutions, we have to choose a reference for the modeling error. This choice has to be done within a larger context, allows for discretion and again is not guided by strict rules like other arts. Furthermore, the reference may shift while getting better model solutions during testing.

A bad model solution may be caused by a bad model – bad choice of properties, poor relations of properties, insufficient discretization, programming errors – or by incorrect model parameters. *Parameters* are those properties which are assumed to be known in advance for a particular problem and are not object to a computation. Under the assumption of a good model, the model parameters can be corrected by a *calibration*. This is based upon appropriate problems from the reality of interest with the known real data. On one hand calibration minimizes the modeling error by adjusting of parameters. On the other hand, *validation* chooses other problems with known real data and assesses the modeling error without adjusting of parameters. Hopefully model solutions are still good.

Regarding reinforced concrete structures, calibrations usually involve the adaption of material parameters like strength and stiffness as part of *material models*. These parameters

are chosen such that the behavior of material specimen observed in experiments is reproduced. A validation is usually performed with structural elements such as bars, beams, plates, and slabs. Computational results of *structural models* are compared with the corresponding experimental data.

This leads to basic peculiarities. Reproducible experiments performed with structural elements are of a small simplified format compared with complex unique buildings. Furthermore, repeated experimental tests with the same nominal parameters exhibit scattering results. Standardized *benchmark tests* carving out different aspects of reinforced concrete behavior are required. Actually a common agreement about such benchmark tests exists only in the first attempts. Regarding a particular problem a corresponding model has to be validated on a case-by-case strategy using adequate experimental investigations. Their choice again has no strict rules as the preceding arts.

Complex proceedings have been sketched hitherto outlining a model of modeling. Some benefit is desirable finally. Thus, a model which passed validations is usable for *predictions*. Structures created along such predictions hopefully prove their worth in the reality of interest.

This textbook covers the range of conceptual models, mathematical models, and numerical models with special attention to reinforced concrete structures. Notes regarding the computational model including available programs and example data are given in Appendix F. A major aspect of the following is modeling of *ultimate limit states*: states with maximum bearable loading or acceptable deformations and displacements in relation to failure. Another aspect is given with *serviceability*: Deformations and in some cases oscillations of structures have to be limited to allow their proper usage and fulfillment of intended services. *Durability* is a third important aspect for building structures: deterioration of materials through, e.g., corrosion, has to be controlled. This is strongly connected to cracking and crack width in the case of reinforced concrete structures. Both topics are also treated in the following.

1.2 Discretization Outline

The finite element method (FEM) is a predominant method to derive numerical models from mathematical models. Its basic theory is described in the remaining sections of this chapter insofar as it is needed for its application to different types of structures with reinforced concrete in the following chapters.

The underlying mathematical model is defined in one-, two-, or three-dimensional fields of space related to a *body* and one-dimensional space of time. A body undergoes deformations during time due to loading. We consider a simple example with a plate defined in 2D space, see Fig. 1.2. Loading is generally defined depending on time whereby time may be replaced by a loading factor in the case of quasistatic problems. Field variables depending on spatial coordinates and time are, e.g., given by the displacements.

- Such fields are discretized by dividing space into *elements* which are connected by *nodes*, see Fig. 1.3a. Elements adjoin but do not overlap and fill out the space of the body under consideration.

- Discretization basically means *interpolation*,, i.e., displacements within an element are interpolated using the values at nodes belonging to the particular element.

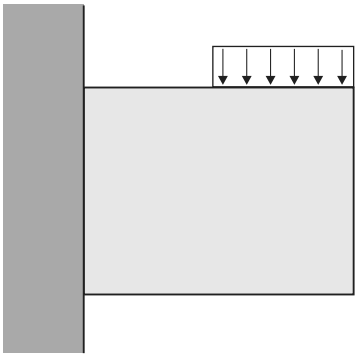

Figure 1.2: Model of a plate.

In the following this will be written as

$$\mathbf{u} = \mathbf{N} \cdot \boldsymbol{v} \tag{1.1}$$

with the displacements $\mathbf{u}$ depending on spatial coordinates and time, a matrix $\mathbf{N}$ of *shape functions* depending on spatial coordinates and a vector $\boldsymbol{v}$ depending on time and collecting all displacements at nodes. The number of components of $\boldsymbol{v}$ is n. It is two times the number of nodes in the case of the plate as the displacement $\mathbf{u}$ has components u_x, u_y. Generally some values of $\boldsymbol{v}$ may be chosen such that the *essential or displacement boundary conditions* of the problem under consideration is fulfilled by the displacements interpolated by Eq. (1.1). This is assumed for the following.

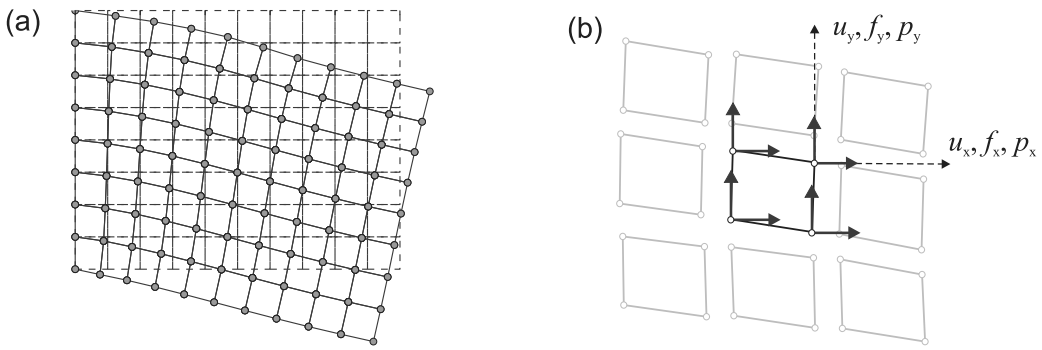

Figure 1.3: (a) Elements and nodes (deformed). (b) Nodal quantities.

Strains are derived from displacements by differentiation with respect to spatial coordinates. In the following, this will be written as

$$\boldsymbol{\epsilon} = \mathbf{B} \cdot \boldsymbol{v} \tag{1.2}$$

with the strains $\boldsymbol{\epsilon}$ depending on spatial coordinates and time, a matrix $\mathbf{B}$ of spatial derivatives of shape functions depending on spatial coordinates and the vector $\boldsymbol{v}$ as has been used in Eq. (1.1). The first examples for Eqs. (1.1, 1.2) will be given in Section 1.3.

- A field variable $\mathbf{u}$ is discretized with Eqs. (1.1, 1.2), i.e., the infinite field in space is reduced into a finite number n of variables in supporting spatial points or nodes which are collected in $\boldsymbol{v}$.

Thereby *kinematic compatibility* should be assured regarding interpolated displacements, i.e., generally spoken a coherence of displacements and deformations should be given.

Strains $\boldsymbol{\epsilon}$ lead to stresses $\boldsymbol{\sigma}$. A *material law* connects both. Material laws for solids are a science in itself. This textbook mainly covers their flavors for reinforced concrete structures. To begin with, such laws are abbreviated with

$$\boldsymbol{\sigma} = f(\boldsymbol{\epsilon}) \tag{1.3}$$

Beyond total values of stress and strain their small changes in time t have to be considered. They are measured with time derivatives

$$\dot{\boldsymbol{\epsilon}} = \frac{\partial \boldsymbol{\epsilon}}{\partial t}, \quad \dot{\boldsymbol{\sigma}} = \frac{\partial \boldsymbol{\sigma}}{\partial t} \tag{1.4}$$

Nonlinear material behavior is mainly formulated as a relation between $\dot{\boldsymbol{\epsilon}}$ and $\dot{\boldsymbol{\sigma}}$. The first concepts about material laws are given in Section 1.4.

An *equilibrium condition* is the third basic element of structural analysis beneath kinematic compatibility and material laws. It is advantageously formulated as principle of virtual work leading to

$$\int_V \delta\boldsymbol{\epsilon}^T \cdot \boldsymbol{\sigma} \, \mathrm{d}V = \int_V \delta\mathbf{u}^T \cdot \mathbf{b} \, \mathrm{d}V + \int_{A_t} \delta\mathbf{u}^T \cdot \mathbf{t} \, \mathrm{d}A \tag{1.5}$$

for quasistatic cases with the volume V of the solid body of interest, its body forces $\mathbf{b}$, its surface A, and its surface tractions $\mathbf{t}$ which are prescribed at a part A_t of the whole boundary A. Furthermore, virtual displacements $\delta\mathbf{u}$ and the corresponding virtual strains $\delta\boldsymbol{\epsilon}$ are introduced. They are arranged as vectors and $\delta\mathbf{u}^T, \delta\boldsymbol{\epsilon}^T$ indicate their transposition into row vectors to have a proper scalar product with $\boldsymbol{\sigma}, \mathbf{b}, \mathbf{t}$ which are also arranged as vectors. Fields of $\mathbf{b}$ and $\mathbf{t}$ are generally prescribed for a problem under consideration while the field of stresses $\boldsymbol{\sigma}$ remains to be determined. Surface tractions $\mathbf{t}$ constitute the *natural* or *force boundary conditions*.

- Stresses $\boldsymbol{\sigma}$ and loadings $\mathbf{b}$, $\mathbf{t}$ are in static equilibrium for the problem under consideration if Eq. (1.5) is fulfilled for arbitrary virtual displacements $\delta\mathbf{u}$ and the corresponding virtual strains $\delta\boldsymbol{\epsilon}$.

Thereby, $\delta\mathbf{u}$ is zero at the part A_u of the whole boundary A with prescribed displacement boundary conditions. Applying the displacement interpolation equation (1.1) to virtual displacements leads to

$$\delta\mathbf{u} = \mathbf{N} \cdot \delta\boldsymbol{v}, \qquad \delta\boldsymbol{\epsilon} = \mathbf{B} \cdot \delta\boldsymbol{v} \tag{1.6}$$

and using this with Eq. (1.5) to

$$\delta\boldsymbol{v}^T \cdot \left[\int_V \mathbf{B}^T \cdot \boldsymbol{\sigma} \, \mathrm{d}V \right] = \delta\boldsymbol{v}^T \cdot \left[\int_V \mathbf{N}^T \cdot \mathbf{b} \, \mathrm{d}V + \int_{A_t} \mathbf{N}^T \cdot \mathbf{t} \, \mathrm{d}A \right] \tag{1.7}$$

with transpositions $\delta\boldsymbol{v}^T, \mathbf{B}^T, \mathbf{N}^T$ of the vector $\delta\boldsymbol{v}$ and the matrices $\mathbf{B}, \mathbf{N}$. As $\delta\boldsymbol{v}$ is arbitrary a *discretized condition of static equilibrium* is derived in the form

$$\mathbf{f} = \mathbf{p} \tag{1.8}$$

with the vector $\mathbf{f}$ of *internal nodal forces* and the vector $\mathbf{p}$ of *external nodal forces*

$$\begin{aligned} \mathbf{f} &= \int_V \mathbf{B}^T \cdot \boldsymbol{\sigma}\, \mathrm{d}V \\ \mathbf{p} &= \int_V \mathbf{N}^T \cdot \mathbf{b}\, \mathrm{d}V + \int_{A_t} \mathbf{N}^T \cdot \mathbf{t}\, \mathrm{d}A \end{aligned} \tag{1.9}$$

Corresponding to the length of the vector $\boldsymbol{v}$ the vectors $\mathbf{f}$, $\mathbf{p}$ have n components.

- By means of $\boldsymbol{\sigma} = \mathbf{f}(\boldsymbol{\epsilon})$ and $\boldsymbol{\epsilon} = \mathbf{B} \cdot \boldsymbol{v}$, Eq. (1.8) constitutes a system of n nonlinear algebraic equations whereby the nodal displacements $\boldsymbol{v}$ have to be determined such that – under the constraint of displacement boundary conditions – internal nodal forces $\mathbf{f}$ are equal to prescribed external nodal forces $\mathbf{p}$.

Nonlinear stress–strain relations, i.e., *physical nonlinearities*, are always an issue for reinforced concrete structures. It is a good practice in nonlinear simulation to start with a linearization to have a reference for the refinements of a conceptual model. *Physical linearity* is described with

$$\boldsymbol{\sigma} = \mathbf{C} \cdot \boldsymbol{\epsilon} \tag{1.10}$$

with a constant material matrix $\mathbf{C}$. Thus, using Eq. (1.2) internal forces $\mathbf{f}$ (Eq. (1.9)) can be formulated as

$$\mathbf{f} = \mathbf{K} \cdot \boldsymbol{v}, \qquad \mathbf{K} = \int_V \mathbf{B}^T \cdot \mathbf{C} \cdot \mathbf{B}\, \mathrm{d}V \tag{1.11}$$

with a constant stiffness matrix $\mathbf{K}$ leading to

$$\mathbf{K} \cdot \boldsymbol{v} = \mathbf{p} \tag{1.12}$$

This allows for a direct determination of nodal displacements which is symbolically written as

$$\boldsymbol{v} = \mathbf{K}^{-1} \cdot \mathbf{p} \tag{1.13}$$

Actually the solution is not determined with a matrix inversion but with more efficient techniques, e.g., Gauss triangularization. Stresses $\boldsymbol{\sigma}$ and strains $\boldsymbol{\epsilon}$ follow with a solution $\boldsymbol{v}$ given. A counterpart of physical linearity is *geometric linearity*:

- Small displacements and geometric linearity are assumed throughout the following if not otherwise stated.

This was a fast track for the finite element method. The rough outline will be filled out in the following. Comprehensive descriptions covering all aspects are given in, e.g., [98], [99], [9], [3]. The special aspects of reinforced concrete structures are treated in [16], [44], [81].

1.3 Elements

Interpolation performed with finite elements will be described with more details in the following. We consider the mechanical behavior of *material points* within a body. A material point is identified by its spatial coordinates. It is convenient to use a different coordinate system simultaneously. First of all, the global *Cartesian coordinate system*, see Appendix C, which is shared by all material points of a body. Thus, a material point is identified by global Cartesian coordinates

$$\mathbf{x} = \begin{pmatrix} x & y & z \end{pmatrix}^T \tag{1.14}$$

in 3D space. In the following, we assume that the space occupied by the body has been divided into finite elements. Thus, a material point may alternatively be identified by the label I of the element it belongs to and its local coordinates

$$\mathbf{r} = \begin{pmatrix} r & s & t \end{pmatrix}^T \tag{1.15}$$

related to a particular *local coordinate system* belonging to the element e. A material point undergoes *displacements*. In the case of translations they are measured in the global Cartesian system by

$$\mathbf{u} = \begin{pmatrix} u & v & w \end{pmatrix}^T \tag{1.16}$$

Displacements in a general sense may also be measured by means of rotations

$$\boldsymbol{\varphi} = \begin{pmatrix} \varphi_x & \varphi_y & \varphi_z \end{pmatrix}^T \tag{1.17}$$

if we consider a material point embedded in some neighborhood of surrounding points. The indices indicate the respective reference axes of rotation.

Isoparametric interpolation will be used in the following. The general interpolation form (Eq. (1.1)) is particularized as

$$\mathbf{u} = \mathbf{N}(\mathbf{r}) \cdot \boldsymbol{v}_e \tag{1.18}$$

whereby the global coordinates of the corresponding material point are given by

$$\mathbf{x} = \mathbf{N}(\mathbf{r}) \cdot \mathbf{x}_e \tag{1.19}$$

The vector $\boldsymbol{v}_e$ collects all nodal displacements of all nodes belonging to the element e and the vector $\mathbf{x}_e$ all global nodal coordinates of that element. Isoparametric interpolation is characterized by the same interpolation for geometry and displacements with the same shape functions $\mathbf{N}(\mathbf{r})$. Global and local coordinates are related by the *Jacobian*

$$\mathbf{J} = \frac{\partial \mathbf{x}}{\partial \mathbf{r}} \tag{1.20}$$

which may be up to a 3×3 matrix for 3D cases. Strains may be derived with displacements related to global coordinates through isoparametric interpolation. Their definition depends on the type of the structural problem. A general formulation

$$\boldsymbol{\epsilon} = \mathbf{B}(\mathbf{r}) \cdot \boldsymbol{v}_e \tag{1.21}$$

is used. Strains $\boldsymbol{\epsilon}$ finally lead to stresses $\boldsymbol{\sigma}$. Examples are given in the following.

– Two-node bar element along a line.

The line is measured by a coordinate x. Each coordinate has a cross section with a cross-sectional area. The *kinematic assumption* of a bar is that every material point in the cross section has the same displacement in the line direction.

A bar element e has nodes I, J with coordinates x_I, x_J. The nodes have the displacements u_I, u_J along the line. The origin of the local coordinate r is placed in the center between the two nodes. Regarding Eqs. (1.18, 1.19) we have

$$\begin{aligned} \mathbf{x} &= \begin{pmatrix} x \end{pmatrix}, \quad \mathbf{u} = \begin{pmatrix} u \end{pmatrix} \\ \mathbf{N} &= \begin{bmatrix} \frac{1}{2}(1-r) & \frac{1}{2}(1+r) \end{bmatrix} \\ \mathbf{x}_e &= \begin{pmatrix} x_I \\ x_J \end{pmatrix}, \quad \boldsymbol{v}_e = \begin{pmatrix} u_I \\ u_J \end{pmatrix} \end{aligned} \tag{1.22}$$

This leads to a scalar Jacobian

$$J = \frac{\partial x}{\partial r} = \frac{L_e}{2} \tag{1.23}$$

Strains are uniaxial and defined by

$$\epsilon = \frac{\partial u}{\partial x} = \frac{\partial u}{\partial r}\frac{\partial r}{\partial x} \tag{1.24}$$

leading to

$$\mathbf{B} = \frac{2}{L_e}\begin{bmatrix} -\frac{1}{2} & \frac{1}{2} \end{bmatrix} \tag{1.25}$$

with a bar length $L_e = x_J - x_I$ and finally, regarding Eq. (1.3), to uniaxial strains and stresses

$$\boldsymbol{\epsilon} = \begin{pmatrix} \epsilon \end{pmatrix}, \quad \boldsymbol{\sigma} = \begin{pmatrix} \sigma \end{pmatrix} \tag{1.26}$$

which are constant along the element.

– Two-node bar element in a plane

The plane is measured by coordinates x, y. The center axis of a bar is a line in this plane. Each point of the center axis again has a cross-sectional area and again the *kinematic assumption* of this bar is that every material point in the cross section has the same displacement in the direction of the center axis.

A bar element e has nodes I, J with coordinates x_I, y_I, x_J, y_J. The nodes have the displacements u_I, v_J, u_I, v_J in a plane. The origin of the local coordinate r is placed in the center between the two nodes. Regarding Eqs. (1.18) and (1.19) we have

$$\begin{aligned} \mathbf{x} &= \begin{pmatrix} x \\ y \end{pmatrix}, \quad \mathbf{u} = \begin{pmatrix} u \\ v \end{pmatrix} \\ \mathbf{N} &= \begin{bmatrix} \frac{1}{2}(1-r) & 0 & \frac{1}{2}(1+r) & 0 \\ 0 & \frac{1}{2}(1-r) & 0 & \frac{1}{2}(1+r) \end{bmatrix} \\ \mathbf{x}_e &= \begin{pmatrix} x_I \\ y_I \\ x_J \\ y_J \end{pmatrix}, \quad \boldsymbol{v}_e = \begin{pmatrix} u_I \\ v_I \\ u_J \\ v_J \end{pmatrix} \end{aligned} \tag{1.27}$$

Uniaxial strain is measured in the direction of the bar's center axis, i.e., in a rotated coordinate system x', y' with x' being aligned to the center axis. The rotation angle α (counterclockwise positive) and the transformation matrix $\mathbf{T}$ for global coordinates and displacements are given by

$$\mathbf{T} = \begin{bmatrix} \cos\alpha & \sin\alpha \\ -\sin\alpha & \cos\alpha \end{bmatrix}, \quad \cos\alpha = \frac{x_J - x_I}{L_e}, \quad \sin\alpha = \frac{y_J - y_I}{L_e} \tag{1.28}$$

with a bar length $L_e = \sqrt{(y_J - y_I)^2 + (x_J - x_I)^2}$. The scalar Jacobian is similar as before

$$J = \frac{\partial x'}{\partial r} = \frac{L_e}{2} \tag{1.29}$$

Strains are again uniaxial and defined by

$$\epsilon = \frac{\partial u'}{\partial x'} = \frac{\partial u'}{\partial r}\frac{\partial r}{\partial x'} \tag{1.30}$$

leading to

$$\mathbf{B} = \frac{2}{L_I}\begin{bmatrix} -\frac{1}{2} & \frac{1}{2} \end{bmatrix} \cdot \begin{bmatrix} \cos\alpha & \sin\alpha & 0 & 0 \\ 0 & 0 & \cos\alpha & \sin\alpha \end{bmatrix} \tag{1.31}$$

regarding Eqs. (1.22_2, 1.28). Uniaxial strains and stresses have a form as given by Eq. (1.26).

– Two-node spring element along a line.

The line is measured by a coordinate x. A spring element e has nodes I, J with coordinates x_I, x_J. The nodes may coincide and have the same coordinates. A *kinematic assumption* for springs may be stated as follows: only the displacement difference of two nodes is relevant irrespective of their original distance.

Springs are an abstract concept and do not occupy a space. They miss material points, local coordinates, and a Jacobian. Thus, regarding Eq. (1.21) it is

$$\boldsymbol{\epsilon} = \begin{pmatrix} \Delta u \end{pmatrix}, \quad \mathbf{B} = \begin{bmatrix} -1 & 1 \end{bmatrix}, \quad \boldsymbol{v}_e = \begin{pmatrix} u_I \\ u_J \end{pmatrix} \tag{1.32}$$

whereby this particular strain $\boldsymbol{\epsilon} = \begin{pmatrix} \Delta u \end{pmatrix}$ corresponds to a difference in displacements of nodes and leads to a force $\boldsymbol{\sigma} = \begin{pmatrix} F \end{pmatrix}$. The relation between Δu and F or spring characteristics may be linear or nonlinear.

– Two-node spring element in a plane.

The plane is measured with coordinates x, y. A spring element e has nodes I, J with coordinates x_I, y_I, x_J, y_J which may again coincide. In analogy to Eq. (1.32)

$$\boldsymbol{\epsilon} = \begin{pmatrix} \Delta u \\ \Delta v \end{pmatrix}, \quad \mathbf{B} = \begin{bmatrix} -1 & -1 & 0 & 0 \\ 0 & 0 & 1 & 1 \end{bmatrix}, \quad \boldsymbol{v}_e = \begin{pmatrix} u_I \\ v_I \\ u_J \\ v_J \end{pmatrix} \tag{1.33}$$

Generalized strain $\boldsymbol{\epsilon}$ leads to a generalized stress

$$\boldsymbol{\sigma} = \begin{pmatrix} F_x \\ F_y \end{pmatrix} \tag{1.34}$$

The relation between $\boldsymbol{\epsilon}$ and $\boldsymbol{\sigma}$ may again be linear or nonlinear. It may be appropriate to transform $\boldsymbol{\epsilon}$ to a rotated coordinate system before evaluating $\boldsymbol{\sigma}$ using a transformation matrix as given by $\mathbf{T}$ in Eq. (1.28). This requires back transformation of $\boldsymbol{\sigma}$ to the original coordinate system with the transposed $\mathbf{T}^T$.

– Four-node continuum element in a plane or *quad element*

The plane is measured with coordinates x, y. A continuum element has nodes I, J, K, L with coordinates $x_i, y_i, i = I, \ldots, L$. They span a quad and are ordered counterclockwise. The following local coordinates are assigned: $I : r_I = -1, s_I = -1$; $J : r_J = 1, s_J = -1$; $K : r_K = 1, s_K = 1$; $L : r_L = -1, s_L = 1$. The *kinematic assumption* of a continuum is that displacements are continuous, i.e., no gaps or overlapping occur. Regarding Eqs. (1.18, 1.19), we have

$$\begin{gathered} \mathbf{x} = \begin{pmatrix} x \\ y \end{pmatrix}, \quad \mathbf{u} = \begin{pmatrix} u \\ v \end{pmatrix} \\ \mathbf{N}_i(r,s) = \frac{1}{4} \begin{bmatrix} (1+r_i r)(1+s_i s) & 0 \\ 0 & (1+r_i r)(1+s_i s) \end{bmatrix} \\ \mathbf{x}_{e,i} = \begin{pmatrix} x_i \\ y_i \end{pmatrix}, \quad \boldsymbol{v}_{e,i} = \begin{pmatrix} u_i \\ v_i \end{pmatrix} \end{gathered} \tag{1.35}$$

with $i = I, \ldots, L$ and

$$\mathbf{x}(r,s) = \sum\nolimits_i \mathbf{N}_i(r,s) \cdot \mathbf{x}_{e,i}, \quad \mathbf{u}(r,s) = \sum\nolimits_i \mathbf{N}_i(r,s) \cdot \boldsymbol{v}_{e,i} \tag{1.36}$$

This leads to a Jacobian matrix

$$\mathbf{J}(r,s) = \begin{bmatrix} \frac{\partial x}{\partial r} & \frac{\partial y}{\partial r} \\ \frac{\partial x}{\partial s} & \frac{\partial y}{\partial s} \end{bmatrix}, \quad J = \det \mathbf{J} \tag{1.37}$$

The Jacobian relates the partial derivatives of a function $\bullet$ with respect to local and global coordinates

$$\begin{pmatrix} \frac{\partial \bullet}{\partial r} \\ \frac{\partial \bullet}{\partial s} \end{pmatrix} = \mathbf{J} \cdot \begin{pmatrix} \frac{\partial \bullet}{\partial x} \\ \frac{\partial \bullet}{\partial y} \end{pmatrix} \quad \rightarrow \quad \begin{pmatrix} \frac{\partial \bullet}{\partial x} \\ \frac{\partial \bullet}{\partial y} \end{pmatrix} = \mathbf{J}^{-1} \cdot \begin{pmatrix} \frac{\partial \bullet}{\partial r} \\ \frac{\partial \bullet}{\partial s} \end{pmatrix} \tag{1.38}$$

with the inverse $\mathbf{J}^{-1}$ of $\mathbf{J}$. Small strains are defined by

$$\boldsymbol{\epsilon} = \begin{pmatrix} \epsilon_x \\ \epsilon_y \\ \gamma_{xy} \end{pmatrix} = \begin{pmatrix} \frac{\partial u}{\partial x} \\ \frac{\partial v}{\partial y} \\ \frac{\partial u}{\partial y} + \frac{\partial v}{\partial x} \end{pmatrix} = \begin{pmatrix} \frac{\partial u}{\partial r}\frac{\partial r}{\partial x} + \frac{\partial u}{\partial s}\frac{\partial s}{\partial x} \\ \frac{\partial v}{\partial r}\frac{\partial r}{\partial y} + \frac{\partial v}{\partial s}\frac{\partial s}{\partial y} \\ \frac{\partial u}{\partial r}\frac{\partial r}{\partial y} + \frac{\partial u}{\partial s}\frac{\partial s}{\partial y} + \frac{\partial v}{\partial r}\frac{\partial r}{\partial x} + \frac{\partial v}{\partial s}\frac{\partial s}{\partial x} \end{pmatrix} \tag{1.39}$$

leading to

$$\boldsymbol{\epsilon}(r,s) = \sum\nolimits_i \mathbf{B}_i(r,s) \cdot \boldsymbol{v}_{e,i} \tag{1.40}$$

with $i = I \dots J$ and

$$\mathbf{B}_i(r,s) = \frac{1}{4}\begin{bmatrix} r_i(1+s_i s)\frac{\partial r}{\partial x} + s_i(1+r_i r)\frac{\partial s}{\partial x} & 0 \\ 0 & r_i(1+s_i s)\frac{\partial r}{\partial y} + s_i(1+r_i r)\frac{\partial s}{\partial y} \\ r_i(1+s_i s)\frac{\partial r}{\partial y} + s_i(1+r_i r)\frac{\partial s}{\partial y} & r_i(1+s_i s)\frac{\partial r}{\partial x} + s_i(1+r_i r)\frac{\partial s}{\partial x} \end{bmatrix} \tag{1.41}$$

The partial derivatives $\partial r/\partial x \dots$ are given the components of the inverse Jacobian $\mathbf{J}^{-1}$. Matrices $\mathbf{N}_i, \mathbf{B}_i$ related to single nodes are assembled in larger matrices to yield $\mathbf{N}, \mathbf{B}$. Finally, Cauchy stresses

$$\boldsymbol{\sigma} = \begin{pmatrix} \sigma_x \\ \sigma_y \\ \sigma_{xy} \end{pmatrix} \tag{1.42}$$

correspond to strains in a plane. Lateral strains ϵ_z or stresses σ_z come into play with the distinction of *plane stress*, that is $\sigma_z = 0$, which may lead to a lateral strain $\epsilon_z \neq 0$, or *plane strain*, that is $\epsilon_z = 0$ which may lead to a lateral stress $\sigma_z \neq 0$. The particular values in the z-direction have to be determined indirectly with a material law, see Section 1.4.

All mentioned stresses and the corresponding strains are conjugate with respect to energy, i.e., the product $\boldsymbol{\sigma} \cdot \dot{\boldsymbol{\epsilon}}$ corresponds to a rate of *internal energy* or a rate of specific internal energy. The concept of *stresses* may be *generalized*:

- Depending on the type of structural element $\boldsymbol{\sigma}$ may stand for components of Cauchy stresses or for components of forces or for components of internal forces in a beam cross section, see Section 3.1.1. *Strains* $\boldsymbol{\epsilon}$ are *generalized* correspondingly in order to lead to internal energy, e.g., including displacements in the case forces or curvature in the case of moments.

A basic property of the aforementioned elements is that they approximate coordinates and displacements by *interpolation*: nodal values and interpolated values are identical at nodes. For instance, for the four-node continuum element we have $\mathbf{u} = \boldsymbol{\upsilon}_{e,i}$ for $r = r_i, s = s_i\, i = I, \dots, L$. This property is shared by all types of finite elements.

Another issue concerns *continuity*: For the four-node continuum element the interpolation is continuous between adjacent elements along their common boundary. One sided first derivatives of interpolation exist for each element along the boundary but are different for each element. Thus, the four-node continuum element has C^0-continuity with these properties. Furthermore, the integrals for internal and external nodal forces (Eq. (1.9)) are evaluable. Other elements may require higher orders of continuity for nodal forces to be integrable.

Finally, the issue of *element locking* has to be mentioned. The four-node continuum element, e.g., does not allow us to model the behavior of incompressible solids. Constraining Eqs. (1.41) with the condition of incompressibility $\epsilon_x + \epsilon_y + \epsilon_z = 0$ makes the element much to stiff if internal nodal forces are exactly integrated [9, 8.4]. First basic hints to treat locking are given in Section 1.7. The locking problem is exemplary treated for shells in Section 8.6.

Only a few element types were touched up to now. Further elements often used are 3D-continuum elements, 2D- and 3D-beam elements, shell elements and slab elements as a special case of shell elements. Furthermore, elements imposing constraints like contact conditions

have become common in practice. For details see, e.g., [3]. Regarding the properties of reinforced concrete more details about 2D-beam elements including Bernoulli beams and Timoshenko beams are given in Section 3.3, about slabs in Section 7.4 and about shells in Chapter 8.

1.4 Material Behavior

From a mechanical point of view, material behavior is primarily focused on strains and stresses. The formal definitions of strains and stresses assume a homogeneous area of matter [64]. Regarding the virgin state of solids their behavior initially can be assumed as linear elastic in nearly all relevant cases. Furthermore, the behavior can be initially assumed as isotropic in many cases, i.e., the reaction of a material is the same in all directions. The concepts of *isotropy* and *anisotropy* are discussed in Section 5.3 with more details.

The following types of elasticity are listed exemplary:

– Uniaxial elasticity

$$\sigma = E \ \epsilon \tag{1.43}$$

with uniaxial stress σ, Young's modulus E, and uniaxial strain ϵ.

– Isotropic plane strain

$$\begin{pmatrix} \sigma_x \\ \sigma_y \\ \sigma_{xy} \end{pmatrix} = \frac{E(1-\nu)}{(1+\nu)(1-2\nu)} \begin{bmatrix} 1 & \frac{\nu}{1-\nu} & 0 \\ \frac{\nu}{1-\nu} & 1 & 0 \\ 0 & 0 & \frac{1-2\nu}{2(1-\nu)} \end{bmatrix} \cdot \begin{pmatrix} \epsilon_x \\ \epsilon_y \\ \gamma_{xy} \end{pmatrix} \tag{1.44}$$

with stress components $\sigma_x, \sigma_y, \sigma_{xy}$, Young's modulus E, Poisson's ratio ν, and strain components $\epsilon_x, \epsilon_y, \gamma_{xy}$. This is a subset of the triaxial isotropic linear elastic law as is described in Section 5.3.

– Isotropic plane stress

$$\begin{pmatrix} \sigma_x \\ \sigma_y \\ \sigma_{xy} \end{pmatrix} = \frac{E}{1-\nu^2} \begin{bmatrix} 1 & \nu & 0 \\ \nu & 1 & 0 \\ 0 & 0 & \frac{1-\nu}{2} \end{bmatrix} \cdot \begin{pmatrix} \epsilon_x \\ \epsilon_y \\ \gamma_{xy} \end{pmatrix} \tag{1.45}$$

ensuring $\sigma_z = 0$ for every combination $\epsilon_x, \epsilon_y, \gamma_{xy}$

– Plane bending

$$M = EJ\,\kappa \tag{1.46}$$

with the moment M, curvature κ, Young's modulus E, and cross-sectional moment of inertia J. This is covered by the concept of generalized stresses with $\boldsymbol{\sigma} = \big(M\big)$ and generalized strains $\boldsymbol{\epsilon} = \big(\kappa\big)$.

Equations (1.43)–(1.45) are a special case of

$$\boldsymbol{\sigma} = \mathbf{C} \cdot \boldsymbol{\epsilon} \tag{1.47}$$

with the constant material stiffness matrix $\mathbf{C}$ describing a linear material behavior. At the latest upon approaching material strength, the behavior becomes physically nonlinear. A simple case is given by the uniaxial elastoplastic law

$$\sigma = \begin{cases} E\,(\epsilon - \epsilon_p) & \text{for } -\epsilon_p \le \epsilon \le \epsilon_p \\ \text{sign}\epsilon\, f_y & \text{otherwise} \end{cases} \tag{1.48}$$

and

$$\dot{\epsilon}_p = \dot{\epsilon} \quad \text{for} \quad |\sigma| = f_y \tag{1.49}$$

with a yield stress f_y (unsigned) and an internal state variable ϵ_p. The *internal state variable* indicates the actual remaining strain upon unloading, i.e., $\sigma = 0$ for $\epsilon = \epsilon_p$. An internal state variable captures the preceding load history. The approach covers elastic loading, yielding, elastic unloading and reloading, ongoing yielding in the opposite uniaxial range. This cycle may be repeated whereby yielding is without hardening. Equation (1.49) is a simple *evolution law* for internal state variables. More details about plasticity are given in Section 5.5.

In the case of nonlinear material equations at least an incremental form

$$\dot{\boldsymbol{\sigma}} = \mathbf{C}_T \cdot \dot{\boldsymbol{\epsilon}} \tag{1.50}$$

should exist with the *tangential material stiffness* $\mathbf{C}_T$, which is no longer constant anymore but might depend on stress, strain, and internal state variables. On occasion the *compliance* is needed, as a counterpart of stiffness, i.e.,

$$\boldsymbol{\epsilon} = \mathbf{D} \cdot \boldsymbol{\sigma} \quad \text{or} \quad \dot{\boldsymbol{\epsilon}} = \mathbf{D}_T \cdot \dot{\boldsymbol{\sigma}} \tag{1.51}$$

whereby compliance matrices are inverses of stiffness matrices: $\mathbf{D} = \mathbf{C}^{-1}$, $\mathbf{D}_T = \mathbf{C}_T^{-1}$.

1.5 Weak Equilibrium and Spatial Discretization

The preceding sections gave an introduction of (1) kinematic compatibility within the context of spatial discretization and of (2) material laws. The third cornerstone of structural mechanics is equilibrium which is formulated in a weak form as a principle of virtual work.

Boundary conditions have to be regarded in advance. Given a point on a boundary of a body, either a displacement boundary condition or a force boundary condition (zero force is also a condition) has to be prescribed for this point. Let us assume that displacements are prescribed with $\bar{\mathbf{u}}$ on surface part A_u, tractions are prescribed with $\bar{\mathbf{t}}$ on surface part A_t while A_u together with A_t contain the whole surface A but do not overlap. Thus, equilibrium is given by

$$\int_V \delta\boldsymbol{\epsilon}^T \cdot \boldsymbol{\sigma}\,\mathrm{d}V + \int_V \delta\mathbf{u}^T \cdot \ddot{\mathbf{u}}\,\varrho \mathrm{d}V = \int_V \delta\mathbf{u}^T \cdot \bar{\mathbf{p}}\,\mathrm{d}V + \int_{A_t} \delta\mathbf{u}^T \cdot \bar{\mathbf{t}}\,\mathrm{d}A \tag{1.52}$$

under the conditions

$$\mathbf{u} = \bar{\mathbf{u}} \ \text{ on } A_u, \quad \delta\mathbf{u} = 0 \ \text{ on } A_u \tag{1.53}$$

and $\delta\mathbf{u}$ arbitrary otherwise. The meaning of the symbols is summarized as follows:

$(\bullet)^T$	transpose of column vector $(\bullet)$ leading to row vector
$\mathbf{u}$	field of displacement vector
$\ddot{\mathbf{u}}$	field of acceleration vector
$\delta\mathbf{u}$	field of test functions or virtual displacement vector
$\delta\boldsymbol{\epsilon}$	field of virtual strain vector corresponding to $\delta\mathbf{u}$
$\boldsymbol{\sigma}$	field of stress vector
ϱ	specific mass
$\bar{\mathbf{p}}$	prescribed field of loads distributed in the body
$\bar{\mathbf{t}}$	prescribed field of tractions distributed over surface of the body
V	body volume
A	body surface
A_u	part of surface with prescribed displacements
A_t	part of surface with prescribed tractions

Formulation (1.52) covers structural dynamics and includes quasistatics as a special case. Concentrated loads are not explicitly included. For mathematically precise formulations also covering generalized variational principles see [96]. All listed parameters have to be considered as generalized. The following evaluations of are listed exemplary:

- In the case of a uniaxial bar, Eq. (1.52) becomes

$$\int_L \delta\epsilon\,\sigma\,A\mathrm{d}x + \int_L \delta u\,\ddot{u}\,\varrho A\mathrm{d}x = \int_L \delta u\,\bar{p}\,\mathrm{d}x + [\delta u\,\bar{t}]_0^L \tag{1.54}$$

  with $0 \le x \le L$ under the conditions

$$u_0 = \bar{u}_0,\ \delta u_0 = 0 \ \text{ and/or } \ u_L = \bar{u}_L,\ \delta u_L = 0 \tag{1.55}$$

  with a cross-sectional area A and a load per length $\bar{p}$ in the bar direction whereby the formulation of the last term indicates the boundary term of a partial integration. Surface tractions degenerate to end forces $\bar{t}$ which are prescribed at either $x = 0$ or $x = L$ (or none, but not both at the same time).

- In the case of a plane Bernoulli beam equation (1.52) becomes

$$\int_L \delta w\,\ddot{w}\,\bar{m}\mathrm{d}x + \int_L \delta\kappa\,M\,\mathrm{d}x = \int_L \delta w\,\bar{p}\,\mathrm{d}x - [\delta\varphi\,\bar{M}]_0^L + [\delta w\,\bar{V}]_0^L \tag{1.56}$$

  with $0 \le x \le L$, the deflection w, the beam's slope φ, moment M, shear force V, a distributed mass $\bar{m}$ per length and a distributed lateral load $\bar{p}$ per length. Two boundary conditions can be given at each end $x = 0$ and $x = L$. There are corresponding pairs $(\varphi,\ M)$ and $(w,\ V)$. Only one quantity out of a pair can be prescribed at a boundary. Furthermore, at least two displacement boundary conditions should be given with at least one deflection $\bar{w}_0$ and/or $\bar{w}_L$.

The principle of virtual work or weak integral forms of equilibrium conditions treat a body as a whole. Strong differential forms consider forces applied to infinitesimally small sections or differentials of a body and lead to differential equations. Both are equivalent from a mechanical point of view. This is exemplary demonstrated for beams in Section 3.2. Weak forms are the starting point for *discretization* with finite elements. This has the following steps regarding Eq. (1.52):

1. Mesh generation

   The respective body has to be to filled with elements. No gaps between elements and no overlapping of elements are allowed in the body's interior. Elements may form facets or polygons on the exterior.

   Proportions and geometric distortions of single element may have a considerable influence on the mathematical approximation error.

2. Spatial interpolation of displacements with Eq. (1.18)

   An infinite number of degrees of freedom $\mathbf{u}$ is reduced to a finite number of nodal degrees of freedom $\boldsymbol{\upsilon}_e$ with *trial functions* according to Eq. (1.18). This leads to discretized strains $\boldsymbol{\epsilon}$ with Eq. (1.21).

3. Spatial interpolation of virtual displacements

   Interpolation of virtual displacements $\delta\mathbf{u}$ is performed with *test functions*. The method of Bubnov–Galerkin is generally used with the same functions as trial functions and test functions implying virtual nodal degrees of freedom $\delta\boldsymbol{\upsilon}_e$

   $$\delta\mathbf{u} = \mathbf{N} \cdot \delta\boldsymbol{\upsilon}_e, \quad \delta\boldsymbol{\epsilon} = \mathbf{B} \cdot \delta\boldsymbol{\upsilon}_e \tag{1.57}$$

   and virtual $\delta\boldsymbol{\epsilon}$ strains are determined in the same way as strains.

4. Evaluation of stresses $\boldsymbol{\sigma}$ from stains $\boldsymbol{\epsilon}$ according to a prescribed material law

   This has to be performed by the integration of the incremental form (Eq. (1.50)). The details depend on the material and structural type and are a major issue in all what follows in this textbook.

5. The evaluation of integrals is performed element by element

   $$\begin{aligned}
   \int_{V_e} \delta\boldsymbol{\epsilon}^T \cdot \boldsymbol{\sigma}\, \mathrm{d}V &= \delta\boldsymbol{\upsilon}_e^T \cdot \mathbf{f}_e, \quad \mathbf{f}_e &&= \int_{V_e} \mathbf{B}^T \cdot \boldsymbol{\sigma}\, \mathrm{d}V \\
   \int_{V_e} \delta\mathbf{u}^T \cdot \ddot{\mathbf{u}}\, \varrho \mathrm{d}V &= \delta\boldsymbol{\upsilon}_e^T \cdot \mathbf{M}_e \cdot \ddot{\boldsymbol{\upsilon}}_e, \quad \mathbf{M}_e &&= \int_{V_e} \mathbf{N}^T \cdot \mathbf{N}\, \varrho \mathrm{d}V \\
   \int_{V_e} \delta\mathbf{u}^T \cdot \bar{\mathbf{p}}\, \mathrm{d}x &= \delta\boldsymbol{\upsilon}_e^T \cdot \bar{\mathbf{p}}_e, \quad \bar{\mathbf{p}}_e &&= \int_{V_e} \mathbf{N}^T \cdot \bar{\mathbf{p}}\, dV \\
   \int_{A_{e,t}} \delta\mathbf{u}^T \cdot \bar{\mathbf{t}}\, \mathrm{d}A &= \delta\boldsymbol{\upsilon}_e^T \cdot \bar{\mathbf{t}}_e, \quad \bar{\mathbf{t}}_e &&= \int_{A_{e,t}} \mathbf{N}^T \cdot \bar{\mathbf{t}}\, \mathrm{d}A
   \end{aligned} \tag{1.58}$$

   with an element index e. This includes the element's *internal nodal forces* $\mathbf{f}_e$, its *mass matrix* $\mathbf{M}_e$ and its *external nodal forces* or loadings $\bar{\mathbf{p}}_e$, $\bar{\mathbf{t}}_e$ which are prescribed. For integration methods, see Section 1.6. Internal nodal forces in the end are functions of nodal displacements $\mathbf{f}_e = \mathbf{f}_e(\boldsymbol{\upsilon}_e)$.

6. Assembling of element contributions into a whole system

   Regarding, e.g., global internal nodal forces $\mathbf{f}$, the vector has entries for every degree of freedom of every global node. On the other hand, every meshing should have a table

which connects an element to the global nodes belonging to it. This table relates the position of the entries in $\mathbf{f}_e$ to a position in $\mathbf{f}$.

As a node generally gets contributions from more than one element, the value of an entry in $\mathbf{f}_e$ has to be *added* to the corresponding entry in $\mathbf{f}$. This is symbolically described by

$$\int_V \delta\boldsymbol{\epsilon}^T \cdot \boldsymbol{\sigma}\, \mathrm{d}V = \delta\boldsymbol{v}^T \cdot \mathbf{f} = \sum\nolimits_e \delta\boldsymbol{v}_e^T \cdot \mathbf{f}_e \tag{1.59}$$

The same argumentation holds for $\delta\boldsymbol{v}_e \to \delta\boldsymbol{v}$, $\boldsymbol{v}_e \to \boldsymbol{v}$, $\mathbf{M}_e \to \mathbf{M}$, $\bar{\mathbf{p}}_e \to \bar{\mathbf{p}}$, $\bar{\mathbf{t}}_e \to \bar{\mathbf{t}}$. Global internal nodal forces in the end are a function of global nodal displacements $\mathbf{f} = \mathbf{f}(\boldsymbol{v})$.

7. Regarding arbitrary values of $\delta\boldsymbol{v}$ a spatially discretized system

$$\mathbf{M} \cdot \ddot{\boldsymbol{v}} + \mathbf{f}(\boldsymbol{v}) = \bar{\mathbf{p}} + \bar{\mathbf{t}} \tag{1.60}$$

finally results with the system's mass matrix $\mathbf{M}$, its internal nodal forces $\mathbf{f}$ and its loadings $\bar{\mathbf{p}}, \bar{\mathbf{t}}$. This is a set of ordinary differential equations of second order in time t for nodal displacements $\boldsymbol{v}$. It might be nonlinear due to the nonlinear dependence of internal nodal forces $\mathbf{f}$ on $\boldsymbol{v}$.

This procedure allows for physical nonlinearities. In the special case of *physical linearity* the linear material stiffness $\boldsymbol{\sigma} = \mathbf{C} \cdot \boldsymbol{\epsilon}$ leads to internal nodal forces

$$\mathbf{f}_e = \int_{V_e} \mathbf{B}^T \cdot \mathbf{C} \cdot \mathbf{B}\, \mathrm{d}V \cdot \boldsymbol{v}_e = \mathbf{K}_e \cdot \boldsymbol{v}_e \tag{1.61}$$

see Eqs. $(1.58)_1$ and (1.21), with a constant element stiffness matrix $\mathbf{K}_e$. Assembling leads to a system stiffness matrix $\mathbf{K}$

$$\mathbf{f}(\boldsymbol{v}) = \mathbf{K} \cdot \boldsymbol{v} \tag{1.62}$$

and regarding Eq. (1.60) to

$$\mathbf{M} \cdot \ddot{\boldsymbol{v}} + \mathbf{K} \cdot \boldsymbol{v} = \bar{\mathbf{p}} + \bar{\mathbf{t}} \tag{1.63}$$

which is a system of linear ordinary differential equations of second order in time t.

To treat physical nonlinearities the system's tangential stiffness is involved. The *tangential stiffness matrix* is needed for the solution of the nonlinear system and furthermore reveals characteristic properties, e.g., regarding stability properties. The tangential stiffness of an element is derived with

$$\mathrm{d}\mathbf{f}_e = \frac{\partial \mathbf{f}_e}{\partial \boldsymbol{v}_e} \cdot \mathrm{d}\boldsymbol{v}_e = \mathbf{K}_{Te} \cdot \mathrm{d}\boldsymbol{v}_e \qquad \text{or} \qquad \dot{\mathbf{f}}_e = \mathbf{K}_{Te} \cdot \dot{\boldsymbol{v}}_e \tag{1.64}$$

with

$$\mathbf{K}_{Te} = \int_{V_e} \mathbf{B}^T \cdot \frac{\partial \boldsymbol{\sigma}}{\partial \boldsymbol{\epsilon}} \cdot \frac{\partial \boldsymbol{\epsilon}}{\partial \boldsymbol{v}_e}\, \mathrm{d}V = \int_{V_e} \mathbf{B}^T \cdot \mathbf{C}_T \cdot \mathbf{B}\, \mathrm{d}V \tag{1.65}$$

see Eqs. $(1.58)_1$, (1.50), and (1.21), and a system tangential stiffness $\mathbf{K}_T$

$$\mathrm{d}\mathbf{f} = \mathbf{K}_T \cdot \mathrm{d}\boldsymbol{v} \qquad \text{or} \qquad \dot{\mathbf{f}} = \mathbf{K}_T \cdot \dot{\boldsymbol{v}} \tag{1.66}$$

Finally, the system (1.60) or (1.63) should be constrained with appropriate conditions regarding $\boldsymbol{v}$ to prevent rigid body displacements.

1.6 Numerical Integration and Solution Methods for Algebraic Systems

The integral formulation of equilibrium conditions requires the evaluation of integrals as given by Eq. (1.58). The evaluation is performed element by element. The integration of a quad element, see Section 1.3, is exemplary discussed in the following. A general function $f(x, y)$ indicates the integrand. The isoparametric quad element has a local coordinate system r, s with $-1 \leq r, s, \leq 1$, see Section 1.3. Thus, integration is performed by

$$\int_{V_I} f(x, y)\, \mathrm{d}V = \int_{-1}^{+1} \int_{-1}^{+1} f(r, s)\, J(r, s)\, b\, \mathrm{d}r\mathrm{d}s \tag{1.67}$$

with the determinant J of the Jacobian, see Eq. (1.37), and a thickness b. As closed analytical forms generally are not available for $f(r, s)$ a *numerical integration* has to be performed

$$\int_{-1}^{+1} \int_{-1}^{+1} f(r, s)\, J(r, s)\, b\, \mathrm{d}r\mathrm{d}s = b \sum_{i=0}^{n_i} \sum_{j=0}^{n_i} \eta_i \eta_j\, f(\xi_i, \xi_j)\, J(\xi_i, \xi_j) \tag{1.68}$$

with integration order n_i, sampling points ξ, and weighting factors η. An appropriate scheme is given by the Gauss integration. Its sampling points and weighting factors are listed in Table 1.1 up to an integration order $n_i = 3$. Weighting factors obey a rule $\sum_{i=0}^{n_i} \eta_i = 2$. Accuracy of integration is a key issue.

- Integration accuracy increases with increasing integration order. On the other hand, numerical integration leads to a major contribution to computational costs.

Gauss integration generally is most efficient compared to other numerical integration schemes: an integration order n_i gives exact results for polynoms of order $2n_i + 1$ disregarding round-off errors, e.g., a uniaxial integration of order 1 with two sampling points exactly integrates a polynomial of the order 3. Alternative numerical integration schemes are given by schemes of Simpson, Newton–Cotes, Lobatto.

Discretization and integration lead to a system of ordinary differential equations of second order in time for unknown nodal displacements $\boldsymbol{v}$, see Eq. (1.60). To begin with a

n_i	ξ_i	η_i
0	0.0	2.0
1	±0.57735 02691 89626	1.0
2	±0.77459 66692 41483	0.55555 55555 55556
	0.0	0.88888 88888 88889
3	±0.86113 63115 94053	0.34785 48451 37454
	±0.33998 10435 84856	0.65214 51548 62546
⋮	⋮	⋮

Table 1.1: Sampling points and weights for Gauss integration (15 digits shown).

quasistatic analysis is considered with $\ddot{\boldsymbol{v}} = 0$ leading to

$$\mathbf{r}(\boldsymbol{v}) = \mathbf{p} - \mathbf{f}(\boldsymbol{v}) = \mathbf{0}, \qquad \mathbf{p} = \bar{\mathbf{p}} + \bar{\mathbf{t}} \tag{1.69}$$

with a *residual* $\mathbf{r}$, internal nodal forces $\mathbf{f}$ depending on displacements $\boldsymbol{v}$ and external nodal loads $\mathbf{p}$, which are assumed to be independent of $\boldsymbol{v}$. The general case is nonlinear dependence of $\mathbf{f}$ on $\boldsymbol{v}$. Thus, the solution of Eq. (1.69) has to be determined by an iteration with a sequence $\boldsymbol{v}^{(0)}, \ldots, \boldsymbol{v}^{(\nu)}$. Regarding an arbitrary iteration step (ν) we have $\mathbf{r}(\boldsymbol{v}^{(\nu)}) \neq 0$ and seek for a correction $\delta\boldsymbol{v}$. A linear Taylor expansion is used as a basic approach

$$\begin{aligned} \mathbf{r}(\boldsymbol{v}^{(\nu)} + \delta\boldsymbol{v}) &\approx \mathbf{r}(\boldsymbol{v}^{(\nu)}) + \mathbf{K}_T^{(\nu)} \cdot \delta\boldsymbol{v} \\ &= 0 \end{aligned} \tag{1.70}$$

with a tangential stiffness matrix, see also Eq. (1.65)

$$\mathbf{K}_T^{(\nu)} = -\left.\frac{\partial \mathbf{r}}{\partial \boldsymbol{v}}\right|_{\boldsymbol{v}=\boldsymbol{v}^{(\nu)}} = \left.\frac{\partial \mathbf{f}}{\partial \boldsymbol{v}}\right|_{\boldsymbol{v}=\boldsymbol{v}^{(\nu)}} \tag{1.71}$$

leading to the *Newton–Raphson method*

$$\begin{aligned} \delta\boldsymbol{v} &= \left[\mathbf{K}_T^{(\nu)}\right]^{-1} \cdot \mathbf{r}(\boldsymbol{v}^{(\nu)}) \\ \boldsymbol{v}^{(\nu+1)} &= \boldsymbol{v}^{(\nu)} + \delta\boldsymbol{v} \end{aligned} \tag{1.72}$$

with (hopefully) an improved value $\boldsymbol{v}^{(\nu+1)}$. Iteration may stop if $\|\mathbf{r}(\boldsymbol{v}^{(\nu+1)})\| \ll 1$ and $\|\delta\boldsymbol{v}\| \ll 1$ with a suitable norm $\|\cdot\|$ transforming a vector into a scalar. The method generally has a fast convergence but is relatively costly. The tangential stiffness matrix has to be computed in every iteration step (ν) and a decomposition in order to solve (LU decomposition instead of inversion) has to be performed on it to determine $\delta\boldsymbol{v}$. Alternative iteration methods use variants of the iteration matrix like the modified Newton–Raphson method or the BFGS method or other quasi-Newton methods [3, 8.4], [9, 6.3],[99, 7]. For more details, see Appendix A.

Iterative methods like Newton–Raphson are embedded in an *incrementally iterative* scheme. Thus, loading is given as a history: $\mathbf{p} = \mathbf{p}(t)$. An appropriate choice is $0 \leq t \leq 1$ for the scaling of the load history time, which is different from real time in the case of a quasistatic analysis. The following steps are performed in the incrementally iterative scheme:

1. Discrete time values t_i are regarded with a time step $\Delta t = t_{i+1} - t_i$ and an initial time $t_0 = 0$. A loading $\mathbf{p}_i = \mathbf{p}(t_i)$ is prescribed for all time steps. The incremental material law (Eq. (1.50))
$$\dot{\boldsymbol{\sigma}}(t) = \mathbf{C}_T \cdot \dot{\boldsymbol{\epsilon}}(t) \tag{1.73}$$
is integrated by a numerical integration of stresses and strains using a trapezoidal rule
$$\begin{aligned} \boldsymbol{\sigma}_{i+1} &= \boldsymbol{\sigma}_i + \Delta t\, [\alpha\dot{\boldsymbol{\sigma}}_{i+1} + (1-\alpha)\,\dot{\boldsymbol{\sigma}}_i] \\ \boldsymbol{\epsilon}_{i+1} &= \boldsymbol{\epsilon}_i + \Delta t\, [\alpha\dot{\boldsymbol{\epsilon}}_{i+1} + (1-\alpha)\,\dot{\boldsymbol{\epsilon}}_i] \end{aligned} \tag{1.74}$$
with $\boldsymbol{\sigma}_i = \boldsymbol{\sigma}(t_i)$, $\boldsymbol{\epsilon}_i = \boldsymbol{\epsilon}(t_i)$ and an integration parameter α. The parameters α, Δt rule stability and accuracy of the numerical approach.

2. The implicit scheme with $\alpha = 1$ is used in the following to gain unconditional stability. Thus, Eqs. (1.73, 1.74) lead to

$$\boldsymbol{\sigma}_{i+1} = \boldsymbol{\sigma}_i + \mathbf{C}_{T,i+1} \cdot (\boldsymbol{\epsilon}_{i+1} - \boldsymbol{\epsilon}_i) \tag{1.75}$$

whereby $\mathbf{C}_{T,i+1}$ indicates dependence of the tangential material stiffness on $\boldsymbol{\sigma}_{i+1}$ and/or $\boldsymbol{\epsilon}_{i+1}$.

3. Unknowns are nodal displacements $\boldsymbol{v}_i = \boldsymbol{v}(t_i)$ leading to strains $\boldsymbol{\epsilon}_i$, stresses $\boldsymbol{\sigma}_i$ and internal nodal forces $\mathbf{f}_i$ except the initial state. This state described by $\boldsymbol{v}_0$, $\boldsymbol{\epsilon}_0$, $\boldsymbol{\sigma}_0$, $\mathbf{f}_0$ is assumed to be known and initial equilibrium is given by $\mathbf{r}_0 = \mathbf{p}_0 - \mathbf{f}_0 = \mathbf{0}$.

4. The solution starts with t_1 and $\boldsymbol{v}_1$ has to be determined. This is performed with an iteration $\boldsymbol{v}_1^{(0)}, \ldots, \boldsymbol{v}_1^{(\nu)}$ with, e.g., the Newton–Raphson method using an initial $\boldsymbol{v}_1^{(0)} = \boldsymbol{v}_0$. The iteration involves $\boldsymbol{\epsilon}_1^{(\nu)}$, $\boldsymbol{\sigma}_1^{(\nu)}$, $\mathbf{C}_{T,1}^{(\nu)}$ according to Eq. (1.75).

5. A converged $\boldsymbol{v}_1$ and the corresponding strains $\boldsymbol{\epsilon}_1$ and stresses $\boldsymbol{\sigma}_1$ serve as a base for t_2 and so on until a target time is reached.

The procedure is illustrated in Fig. 1.4 and combined with integration according to Eq. (1.58) and assembling according to Eq. (1.59). The time t serves as a loading parameter in the quasistatic case. A scaling of time, i.e., multiplying time with a constant factor in each occurrence, does not have any influence upon the results.

This starts to become different with a *transient analysis*. A material behavior like creep, see Section 2.2, has to be regarded as transient. Such a behavior is modeled by incorporating viscosity [64, 6.4]. Thus, the incremental material law (Eq. (1.73)) is extended as

$$\dot{\boldsymbol{\sigma}} = \mathbf{C}_T \cdot \dot{\boldsymbol{\epsilon}} + \boldsymbol{\Sigma} \tag{1.76}$$

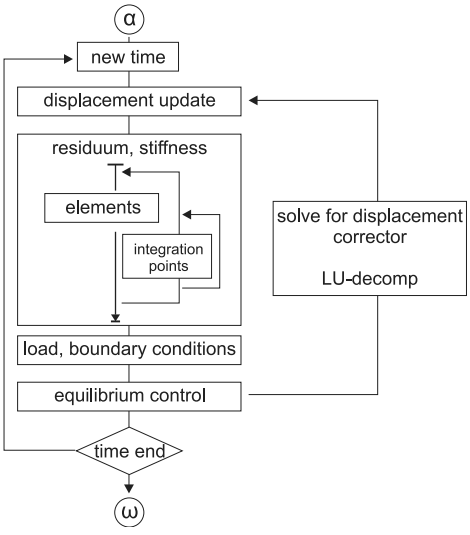

Figure 1.4: Flow of displacement-based nonlinear calculation.

with an additional term $\boldsymbol{\Sigma}$ depending on stress $\boldsymbol{\sigma}(t)$ and strain $\boldsymbol{\epsilon}(t)$. In a similar way as done with Eq. (1.73) leading to Eq. (1.75) this is integrated with

$$\boldsymbol{\sigma}_{i+1} = \boldsymbol{\sigma}_i + \mathbf{C}_{T,i+1} \cdot (\boldsymbol{\epsilon}_{i+1} - \boldsymbol{\epsilon}_i) + \Delta t\, \boldsymbol{\Sigma}_{i+1} \tag{1.77}$$

Internal nodal forces are determined according to Eq. $(1.58)_1$

$$\mathbf{f}_{i+1} = \int_V \mathbf{B}^T \cdot \boldsymbol{\sigma}_{i+1}\, \mathrm{d}V = \mathbf{f}_i + \mathbf{K}_{T,i+1} \cdot \Delta\boldsymbol{\upsilon} + \Delta t\, \bar{\mathbf{f}}_{i+1} \tag{1.78}$$

with element index e omitted and $\Delta\boldsymbol{\upsilon} = \boldsymbol{\upsilon}_{i+1} - \boldsymbol{\upsilon}_i$ and

$$\begin{aligned} \mathbf{f}_i &= \int_V \mathbf{B}^T \cdot \boldsymbol{\sigma}_i\, \mathrm{d}V \\ \mathbf{K}_{T,i+1} &= \int_V \mathbf{B}^T \cdot \mathbf{C}_{T,i+1} \cdot \mathbf{B}\, \mathrm{d}V \\ \bar{\mathbf{f}}_{i+1} &= \int_V \mathbf{B}^T \cdot \boldsymbol{\Sigma}_{i+1}\, \mathrm{d}V \end{aligned} \tag{1.79}$$

The contributions $\mathbf{K}_{T,i+1}, \bar{\mathbf{f}}_{i+1}$ may involve nonlinearities due to the dependence of $\mathbf{C}_{T,i+1}, \boldsymbol{\Sigma}_{i+1}$ on strains and stresses. Equilibrium at a time t_{i+1} has the condition

$$\begin{aligned} \mathbf{r}_{i+1} &= \mathbf{p}_{i+1} - \mathbf{f}_{i+1} \\ &= \mathbf{p}_{i+1} - \mathbf{f}_i - \mathbf{K}_{T,i+1} \cdot \Delta\boldsymbol{\upsilon} - \Delta t\, \bar{\mathbf{f}}_{i+1} \\ &= \mathbf{0} \end{aligned} \tag{1.80}$$

according to Eqs. (1.69, 1.78). We apply the Newton–Raphson method (Eq. (1.72)) to solve this system of algebraic equations within in incrementally iterative scheme, see Eq. (1.72). An extended tangential stiffness, see Eq. (1.71), is given by

$$\mathbf{A}^{(\nu)}_{T,i+1} = \mathbf{K}^{(\nu)}_{T,i+1} + \Delta t\, \left.\frac{\partial \bar{\mathbf{f}}}{\partial \boldsymbol{\upsilon}}\right|_{\boldsymbol{\upsilon}=\boldsymbol{\upsilon}^{(\nu)}_{i+1}} \tag{1.81}$$

with the iteration counter (ν) leading to an iteration scheme

$$\boldsymbol{\upsilon}^{(\nu+1)}_{i+1} = \boldsymbol{\upsilon}^{(\nu)}_{i+1} + \left[\mathbf{A}^{(\nu)}_{T,i+1}\right]^{-1} \cdot \mathbf{r}^{(\nu+1)}_{i+1} \tag{1.82}$$

The exact formulation of the extended tangential stiffness depends on the particular form of $\bar{\mathbf{f}}$ or $\boldsymbol{\Sigma}$, respectively. In the case of time steps Δt being small is $\mathbf{A}^{(\nu)}_T \approx \mathbf{K}^{(\nu)}_T$.

A particular case is given by the viscoelasticity of materials, see Section 2.2, leading to

$$\boldsymbol{\Sigma} = \mathbf{V} \cdot \boldsymbol{\epsilon} - \mathbf{W} \cdot \boldsymbol{\sigma} \tag{1.83}$$

with constant material terms $\mathbf{V}$, $\mathbf{W}$, see Eq. (2.27). Thus, $\boldsymbol{\Sigma}_{i+1} = \mathbf{V} \cdot \boldsymbol{\epsilon}_{i+1} - \mathbf{W} \cdot \boldsymbol{\sigma}_{i+1}$ and stress from Eq. (1.77) becomes

$$\boldsymbol{\sigma}_{i+1} = \boldsymbol{\sigma}_i + \mathbf{C}_{T,i+1} \cdot (\boldsymbol{\epsilon}_{i+1} - \boldsymbol{\epsilon}_i) + \Delta t\, \mathbf{V} \cdot \boldsymbol{\epsilon}_{i+1} - \Delta t\, \mathbf{W} \cdot \boldsymbol{\sigma}_{i+1} \tag{1.84}$$

leading to

$$\boldsymbol{\sigma}_{i+1} = [\mathbf{I} + \Delta t\, \mathbf{W}]^{-1} \cdot \Big([\mathbf{C}_{T,i+1} + \Delta t\, \mathbf{V}] \cdot (\boldsymbol{\epsilon}_{i+1} - \boldsymbol{\epsilon}_i) + \boldsymbol{\sigma}_i + \Delta t\, \mathbf{V} \cdot \boldsymbol{\epsilon}_i \Big) \tag{1.85}$$

with the unit matrix $\mathbf{I}$. Internal nodal forces according to Eq. $(1.58)_1$ are given by

$$\mathbf{f}_{i+1} = \int_V \mathbf{B}^T \cdot \boldsymbol{\sigma}_{i+1}\, \mathrm{d}V = \bar{\mathbf{f}}_i + \bar{\mathbf{K}}_{T,i+1} \cdot \Delta \boldsymbol{v} \tag{1.86}$$

with $\Delta \boldsymbol{v}$ as before and

$$\begin{aligned} \bar{\mathbf{f}}_i &= [\mathbf{I} + \Delta t\, \mathbf{W}]^{-1} \int_V \mathbf{B}^T \cdot (\boldsymbol{\sigma}_i + \Delta t\, \mathbf{V} \cdot \boldsymbol{\epsilon}_i)\, \mathrm{d}V \\ \bar{\mathbf{K}}_{T,i+1} &= [\mathbf{I} + \Delta t\, \mathbf{W}]^{-1} \int_V \mathbf{B}^T \cdot [\mathbf{C}_{T,i+1} + \Delta t\, \mathbf{V}] \cdot \mathbf{B}\, \mathrm{d}V \end{aligned} \tag{1.87}$$

The residual, see Eq. (1.80), is given by

$$\mathbf{r}_{i+1} = \mathbf{p}_{i+1} - \bar{\mathbf{f}}_i - \bar{\mathbf{K}}_{T,i+1} \cdot \Delta \boldsymbol{v} \tag{1.88}$$

leading to an iteration scheme

$$\boldsymbol{v}_{i+1}^{(\nu+1)} = \boldsymbol{v}_{i+1}^{(\nu)} + \Big[\bar{\mathbf{K}}_{T,i+1}^{(\nu)} \Big]^{-1} \cdot \mathbf{r}_{i+1}^{(\nu+1)} \tag{1.89}$$

All quantities at time t_i can assumed to be known within a time stepping scheme. A potential source of nonlinearity is still given by $\mathbf{C}_{T,i+1}$. Formulation (1.87) is used as solution method for Examples 2.2 and 3.3.

Real time t is also a key factor for a *dynamic analysis* regarding inertia. Based on Eq. (1.60) we have in analogy to Eq. (1.69)

$$\mathbf{r} = \mathbf{p}(t) - \mathbf{M} \cdot \ddot{\boldsymbol{v}} - \mathbf{f} = 0, \qquad \mathbf{p}(t) = \bar{\mathbf{p}}(t) + \bar{\mathbf{t}}(t) \tag{1.90}$$

whereby the loading $\mathbf{p}$ is a prescribed function of the time t. The displacements $\boldsymbol{v}(t)$ and all derived values (velocities $\dot{\boldsymbol{v}}(t)$, accelerations $\ddot{\boldsymbol{v}}(t)$, internal nodal forces $\mathbf{f}$) are unknown before solution. Equation (1.90) is discretized in the spatial domain, but not yet in the time domain, i.e., it is system of ordinary differential equations of second order in time. Beneath displacement boundary conditions this problem needs initial conditions for the displacements $\boldsymbol{v}_0 = \boldsymbol{v}(0)$ and velocities $\dot{\boldsymbol{v}}_0 = \dot{\boldsymbol{v}}(0)$.

A widespread approach for the *temporal discretization* of acceleration together with velocities is given in the *Newmark method*

$$\begin{aligned} \dot{\boldsymbol{v}}_{i+1} &= \dot{\boldsymbol{v}}_i + \Delta t \Big[\gamma \ddot{\boldsymbol{v}}_{i+1} + (1-\gamma) \ddot{\boldsymbol{v}}_i \Big] \\ \boldsymbol{v}_{i+1} &= \boldsymbol{v}_i + \Delta t\ \dot{\boldsymbol{v}}_i + \Delta t^2 \Big[\beta \ddot{\boldsymbol{v}}_{i+1} + (\tfrac{1}{2} - \beta) \ddot{\boldsymbol{v}}_i \Big] \end{aligned} \tag{1.91}$$

with $\boldsymbol{v}_{i+1} = \boldsymbol{v}(t_{i+1})$, $\dot{\boldsymbol{v}}_{i+1} = \dot{\boldsymbol{v}}(t_{i+1})$, $\ddot{\boldsymbol{v}}_{i+1} = \ddot{\boldsymbol{v}}(t_{i+1})$ a time step length $\Delta t = t_{i+1} - t_i$ and integration parameters γ, β. Equations (1.91) are solved for the acceleration and velocity in time step $i+1$. We get

$$\ddot{\boldsymbol{v}}_{i+1} = \frac{1}{\beta \Delta t^2} \left[\boldsymbol{v}_{i+1} - \tilde{\boldsymbol{v}}_{i+1} \right] \tag{1.92}$$

with an auxiliary quantity

$$\tilde{\boldsymbol{v}}_{i+1} = \boldsymbol{v}_i + \Delta t \;\; \dot{\boldsymbol{v}}_i + \frac{\Delta t^2}{2} \left(1 - 2\beta\right) \ddot{\boldsymbol{v}}_i \tag{1.93}$$

and the velocity

$$\dot{\boldsymbol{v}}_{i+1} = \frac{\gamma}{\beta \Delta t} \left[\boldsymbol{v}_{i+1} - \boldsymbol{v}_i\right] + \left(1 - \frac{\gamma}{\beta}\right) \dot{\boldsymbol{v}}_i + \Delta t \left(1 - \frac{\gamma}{2\beta}\right) \ddot{\boldsymbol{v}}_i \tag{1.94}$$

Finally, dynamic equilibrium equation (1.90) is applied for the time step $i + 1$ with the acceleration according to Eq. (1.92):

$$\mathbf{r}_{i+1} = \mathbf{p}_{i+1} - \frac{1}{\beta \Delta t^2} \mathbf{M} \cdot \left[\boldsymbol{v}_{i+1} - \tilde{\boldsymbol{v}}_{i+1}\right] - \mathbf{f}_{i+1} = 0 \tag{1.95}$$

With the given parameters $\gamma, \beta, \Delta t$, a given previous state $\boldsymbol{v}_i, \dot{\boldsymbol{v}}_i, \ddot{\boldsymbol{v}}_i$, given mass matrix $\mathbf{M}$ and load $\mathbf{p}_{i+1}$, Eq. (1.95) has to be solved for $\boldsymbol{v}_{i+1}$ whereby the dependence of $\mathbf{f}_{i+1}$ on $\boldsymbol{v}_{i+1}$ is crucial and might be nonlinear.

We apply again the Newton–Raphson method (Eq. (1.72)). An extended tangential stiffness, see Eq. (1.71), is given by

$$\mathbf{A}_T^{(\nu)} = \frac{1}{\beta \Delta t^2} \mathbf{M} + \left.\frac{\partial \mathbf{f}}{\partial \boldsymbol{v}}\right|_{\boldsymbol{v} = \boldsymbol{v}_{i+1}^{(\nu)}} = \frac{1}{\beta \Delta t^2} \mathbf{M} + \mathbf{K}_T^{(\nu)} \tag{1.96}$$

leading to an iteration scheme

$$\boldsymbol{v}_{i+1}^{(\nu+1)} = \boldsymbol{v}_{i+1}^{(\nu)} + \left[\mathbf{A}_T^{(\nu)}\right]^{-1} \cdot \left(\mathbf{p}_{i+1} - \frac{1}{\beta \Delta t^2} \mathbf{M} \cdot \left(\boldsymbol{v}_{i+1}^{(\nu)} - \tilde{\boldsymbol{v}}_{i+1}\right) - \mathbf{f}_{i+1}^{(\nu)}\right) \tag{1.97}$$

This includes the linear case with

$$\mathbf{f}_{i+1}^{(\nu)} = \mathbf{K} \cdot \boldsymbol{v}_{i+1}^{(\nu)}, \qquad \mathbf{A}_T^{(\nu)} = \mathbf{A} = \frac{1}{\beta \Delta t^2} \mathbf{M} + \mathbf{K} \tag{1.98}$$

and Eq. (1.97) simplifies to

$$\boldsymbol{v}_{i+1} = \mathbf{A}^{-1} \cdot \left(\mathbf{p}_{i+1} + \frac{1}{\beta \Delta t^2} \mathbf{M} \cdot \tilde{\boldsymbol{v}}_{i+1}\right) \tag{1.99}$$

with no iteration necessary [2, 9.2.4]. Numerical integration parameters γ, β rule *consistency* and *numerical stability* of the method.

- Stability means that an amount of error introduced in a certain step due to a finite time step length Δt is not is not increased in the subsequent steps.
- Consistency means that the iteration scheme converges to the differential equation for $\Delta t \to 0$.

Stability and consistency are necessary to ensure that the error of the numerical method remains within some bounds for a finite time step length Δt. A choice $\beta = \frac{1}{4}, \gamma = \frac{1}{2}$ is reasonable for the Newmark method to reach consistency and stability [2, 9.4].

This section completes the basic discussion of procedures as they are directly used to solve problems of reinforced concrete structures. The following last section of this chapter touches some theoretical background regarding the finite element method.

1.7 Convergence

The major contribution to the mathematical approximation error, see Section 1.1, is the discretization error arising from the difference between mathematical and numerical model, see Fig. 1.1. This difference should become smaller with a mesh refinement, i.e., the numerical model should *converge* with respect to the underlying mathematical model. Under the assumption of geometrical and physical linearity the convergence behavior of the finite element method can be analyzed theoretically. Quasistatic problems are considered in the following.

The following mathematical symbols are used in this section:

$\forall$	for all
$\in$	element of
$\subset$	subset of
$\exists$	it exists
$\cap$	intersection
$\cup$	union

Given a linear material law

$$\boldsymbol{\sigma} = \mathbf{C} \cdot \boldsymbol{\epsilon} \tag{1.100}$$

the condition of weak, integral equilibrium equation (1.52), can be written as

$$\int_V \delta\boldsymbol{\epsilon}^T \cdot \mathbf{C} \cdot \boldsymbol{\epsilon} \, \mathrm{d}V = \int_V \delta\mathbf{u}^T \cdot \bar{\mathbf{p}} \, \mathrm{d}V + \int_{A_t} \delta\mathbf{u}^T \cdot \bar{\mathbf{t}} \, \mathrm{d}A \tag{1.101}$$

with a given body geometry V and given values for $\mathbf{C}$, $\bar{\mathbf{p}}$ and $\bar{\mathbf{t}}$. The boundary A of V is composed of A_u and A_t whereby $A = A_t \cup A_u$ and $A_t \cap A_u = 0$. Displacement boundary conditions or *Dirichlet conditions* are prescribed on A_u and force boundary conditions or *Neumann conditions* on A_t with $\bar{\mathbf{t}} = \mathbf{n} \cdot \boldsymbol{\sigma}$ with the boundary's normal $\mathbf{n}$. Displacement boundary conditions have to prevent rigid body motions.

Generalized strains $\boldsymbol{\epsilon}, \delta\boldsymbol{\epsilon}$ are derived from the generalized displacements $\mathbf{u}, \delta\mathbf{u}$ by a differential operator depending on the type of the structural problem under consideration. The trial functions according to Eq. (1.18) and test functions according to Eq. (1.57) are assumed to belong to a Sobolev function space H ($\rightarrow$ square integrable functions [2, 4.3.4]) defined over the body V and to fulfill the displacement boundary conditions.

Equation (1.101) can be written in a general form as

$$a(\mathbf{u}, \mathbf{v}) = (\mathbf{f}, \mathbf{v}) \quad \forall \mathbf{v} \in H \tag{1.102}$$

with a symmetric, bilinear operator $a(\cdot, \cdot)$, a further linear operator $(\mathbf{f}, \cdot)$, and $\mathbf{v}$ formally replacing $\delta\mathbf{u}$. This has the following properties:

– Symmetry

$$a(\mathbf{u}, \mathbf{v}) = a(\mathbf{v}, \mathbf{u}) \tag{1.103}$$

– Bilinearity

$$\begin{aligned} a(\gamma_1\mathbf{u}_1 + \gamma_2\mathbf{u}_2, \mathbf{v}) &= \gamma_1 a(\mathbf{u}_1, \mathbf{v}) + \gamma_2 a(\mathbf{u}_2, \mathbf{v}) \\ a(\mathbf{u}, \gamma_1\mathbf{v}_1 + \gamma_2\mathbf{v}_2) &= \gamma_1 a(\mathbf{u}, \mathbf{v}_1) + \gamma_2 a(\mathbf{u}, \mathbf{v}_2) \end{aligned} \tag{1.104}$$

– Linearity

$$(\mathbf{f}, \gamma_1 \mathbf{v}_1 + \gamma_2 \mathbf{v}_2) = \gamma_1 (\mathbf{f}, \mathbf{v}_1) + \gamma_2 (\mathbf{f}, \mathbf{v}_2) \tag{1.105}$$

A *norm* maps a function $\mathbf{v}$ into a nonnegative number. Sobolev norms $||\mathbf{v}||_i$ of order i are used in this context [2, 4.3.4,(4.76)]. Sobolev norms are built from integration of squares of functions and squares of their derivatives up to order i. It is assumed that $i = 1$ is appropriate for the following. It can then be shown that a has the properties

– Continuity

$$\exists\, M > 0 : \quad |a(\mathbf{v}_1, \mathbf{v}_2)| \leq M \, \|\mathbf{v}_1\|_1 \, \|\mathbf{v}_2\|_1 \quad \forall \mathbf{v}_1, \mathbf{v}_2 \in H \tag{1.106}$$

– Ellipticity

$$\exists\, \alpha > 0 : \quad a(\mathbf{v}, \mathbf{v}) \geq \alpha \, \|\mathbf{v}\|_1^2 \quad \forall \mathbf{v} \in H \tag{1.107}$$

whereby M, α depend on problem type and material values but not on $\mathbf{v}_1, \mathbf{v}_2, \mathbf{v}$.

Due to Eq. (1.107) $a(\mathbf{v}, \mathbf{v}) \geq 0$, i.e., a is a norm and may be physically interpreted as *energy*. It is twice the internal strain energy. It can be shown that the problem Eq. (1.102) – i.e., determine a function $\mathbf{u} \in H$ such that Eq. (1.102) is fulfilled for all $\mathbf{v} \in H$ – has a unique solution $\mathbf{u}$, see, e.g., [2, 4.3]. This is the *exact solution* of the mathematical model, see Fig. 1.1.

Discretization uses trial and test functions $\mathbf{u}_h, \mathbf{v}_h \in H_h$ of a subset $H_h \subset H$ based upon the concept of meshes and interpolation with elements and nodes, see Section 1.3. To simplify the derivations, a uniform mesh of elements is assumed with a mesh size parameter h, e.g., a diameter or length of a generic element. For nonuniform meshes see [2, 4.3.5]. The *approximate solution* $\mathbf{u}_h \in H_h$ of Eq. (1.102) is determined by

$$a(\mathbf{u}_h, \mathbf{v}_h) = (\mathbf{f}, \mathbf{v}_h) \quad \forall \mathbf{v}_h \in H_h \tag{1.108}$$

The difference between approximate and exact solution gives the *discretization error*

$$\mathbf{e}_h = \mathbf{u} - \mathbf{u}_h \tag{1.109}$$

The approximation $\mathbf{u}_h$ is known for H_h given, it can be determined according to the procedure described in Section 1.5. The error $\mathbf{e}_h$ has to be estimated. The approximate solution has the following properties:

– Orthogonality of error, see [2, (4.86)]

$$a(\mathbf{e}_h, \mathbf{v}_h) = 0 \quad \forall \mathbf{v}_h \in H_h \tag{1.110}$$

– Energy of approximation is smaller than exact energy, see [2, (4.89)]

$$a(\mathbf{u}_h, \mathbf{u}_h) \leq a(\mathbf{u}, \mathbf{u}) \tag{1.111}$$

– Energy of error is minimized, see [2, (4.91)]

$$a(\mathbf{e}_h, \mathbf{e}_h) \leq a(\mathbf{u} - \mathbf{v}_h, \mathbf{u} - \mathbf{v}_h) \quad \forall \mathbf{v}_h \in H_h \tag{1.112}$$

Combination of Eqs. (1.107), (1.112), and (1.106) leads to

$$\begin{aligned} \alpha \left\| \mathbf{e}_h \right\|_1^2 &= \alpha \left\| \mathbf{u} - \mathbf{u}_h \right\|_1^2 \leq a(\mathbf{e}_h, \mathbf{e}_h) \\ &= \inf_{\mathbf{v}_h \in H_h} a(\mathbf{u} - \mathbf{v}_h, \mathbf{u} - \mathbf{v}_h) \leq M \inf_{\mathbf{v}_h \in H_h} \left\| \mathbf{u} - \mathbf{v}_h \right\|_1^2 \end{aligned} \tag{1.113}$$

where inf is infimum, the largest lower bound[1]. This is rewritten as

$$\left\| \mathbf{u} - \mathbf{u}_h \right\|_1 \leq c \;\; d(\mathbf{u}, H_h) \tag{1.114}$$

with

$$d(\mathbf{u}, H_h) = \inf_{\mathbf{v}_h \in H_h} \left\| \mathbf{u} - \mathbf{v}_h \right\|_1, \quad c = \sqrt{M/\alpha} \tag{1.115}$$

d is a "distance" of functions in H_h to the exact solution $\mathbf{u}$, c depends on the structural problem type and the values of its parameters, but *not* on H_h.

- *Convergence* means $\mathbf{u}_h \to \mathbf{u}$ or $\left\| \mathbf{u} - \mathbf{u}_h \right\|_1 \to 0$ with mesh size $h \to 0$.

Convergence can be reached with an appropriate selection of function spaces H_h whereby reducing the distance $d(\mathbf{u}, H_h)$.

A more precise statement is possible using interpolation theory. This introduces the interpolant[2] $\mathbf{u}_i \in H_h$ of the exact solution $\mathbf{u}$. Complete polynomials[3] of degree k are used for discretization and interpolation. Interpolation theory estimates the interpolation error with

$$\left\| \mathbf{u} - \mathbf{u}_i \right\|_1 \leq \hat{c}\, h^k \left\| \mathbf{u} \right\|_{k+1} \tag{1.116}$$

with the mesh size h and a constant $\hat{c}$ which is independent of h [2, (4.99)]. $\left\| \mathbf{u} \right\|_{k+1}$ is the $k+1$-order Sobolev norm of the exact solution. On the other hand a relation $\inf_{\mathbf{v}_h \in H_h} \left\| \mathbf{u} - \mathbf{v}_h \right\|_1 \leq \left\| \mathbf{u} - \mathbf{u}_i \right\|_1$ must hold as $\mathbf{u}_i \in H_h$. Using this and Eqs. (1.114, 1.116) yields

$$\left\| \mathbf{u} - \mathbf{u}_h \right\|_1 \leq c\hat{c}\, h^k \left\| \mathbf{u} \right\|_{k+1} \tag{1.117}$$

The value $c\hat{c}$ can be merged to c, which depends on the structural problem type and the values of its parameters, but *not* on h. A further merging of c and $\left\| \mathbf{u} \right\|_{k+1}$ leads to the well-known formulation

$$\left\| \mathbf{u} - \mathbf{u}_h \right\|_1 \leq c\, h^k \tag{1.118}$$

whereby c depends on the structural problem type, the values of its parameters and the norm of the exact solution.

The following conditions for convergence can be derived [2, 4.3.2]:

– A prerequisite is theoretical integrability of all quantities. This leads to requirements for the integrands of the energy a and the arguments of the Sobolov norms, which are $\mathbf{u}_h, \mathbf{v}_h, \mathbf{u}$ or derivatives thereof.

  This corresponds to the requirement of *compatibility* or *continuity* – with a different meaning compared to Eq. (1.106) –, respectively, of finite element interpolation functions – generally displacement interpolations – along inter element boundaries.

[1] $\left\| \mathbf{u} - \mathbf{v}_h \right\|_1, \mathbf{v}_h \in H_h$ is a subset of real numbers. $\inf_{\mathbf{v}_h \in H_h} \left\| \mathbf{u} - \mathbf{v}_h \right\|_1$ is the largest number less or equal to the numbers in this subset.

[2] $\mathbf{u}$ and $\mathbf{u}_i$ coincide at nodes, but generally not apart from nodes. Generally is $\mathbf{u}_i \neq \mathbf{u}_h$.

[3] A polynomial in x, y is complete of order 1 if it includes x, y, complete of order 2 if of order 1 and including x^2, xy, y^2, complete of order 3 if complete of order 2 and including x^3, x^2y, xy^2, y^3 and so on.

– According to Eq. (1.118), a sequence of approximate solutions $\mathbf{u}_h$ with $h \to 0$ will converge[4] with respect to $\|\mathbf{u} - \mathbf{u}_h\|_1$ if $k \geq 1$.

  The case $k = 1$ is covered by the *patch test*, i.e., the ability to model fields with constant first derivatives of finite element interpolation functions in arbitrary element configurations [9, 8.3.2]).

– The convergence rate will be higher for larger values of k, i.e., if the finite element interpolation has a higher order of completeness.

Limitations of these arguments have to be mentioned. Under certain conditions the coefficient c may become so large that acceptable solutions, i.e., a sufficiently small value $||\mathbf{u} - \mathbf{u}_h||$, cannot be reached with realizable values h small enough. A particular occurrence is given by locking of approximate solutions with incompressible or nearly incompressible materials.

The locking problem motivates the inclusion of extended weak forms of equilibrium conditions. Equations (1.101, 1.102) are weak forms of *displacement based methods*, as a solution is given by a displacement field. Strains and stresses are derived from this solution. Extended weak forms allow us to involve fields for stresses and strains as independent solution variables. Most prominent are the *principles of Hu-Washizu* and *Hellinger-Reissner* [2, 4.4.2]. An abstract extended problem definition analogous to Eq. (1.108) is given by [3, (16)]

$$\begin{array}{rcll} a(\mathbf{u}_h, \mathbf{v}_h) + b(\boldsymbol{\epsilon}_h, \mathbf{v}_h) & = & (\mathbf{f}, \mathbf{v}_h) & \forall \mathbf{v}_h \in H_h \\ b(\mathbf{w}_h, \mathbf{u}_h) - c(\boldsymbol{\epsilon}_h, \mathbf{e}_h) & = & 0 & \forall \mathbf{w}_h \in W_h \end{array} \tag{1.119}$$

in which a, c are symmetric bilinear forms, b is a bilinear form, f is a linear form, H_h, W_h are appropriate functions spaces, $\mathbf{u}_h \in H_h, \boldsymbol{\epsilon}_h \in W_h$ are the approximate solutions. In most cases $\boldsymbol{\epsilon}_h$ stands for an independent field of strains or stresses. Such an approach requires an extension of the foregoing discussion related to displacement based methods including the widely referenced *inf-sup condition* [3]. The provided framework to include independent interpolations for displacements, strains, and stresses may avoid locking problems to a large degree. Cases of locking risks will be discussed individually if necessary in the following.

The foregoing discussion is related to linear problems. They cannot be strictly applied to nonlinear problems – physically nonlinear and/or geometrically nonlinear. But the conclusions to be drawn regarding element selection and discretization should also be considered for nonlinear and dynamic problems.

[4] Converge with respect to first order Sobolev norm $\|\mathbf{u} - \mathbf{u}_h\|_1$ may not be sufficient if generalized strains are derived from higher derivatives of displacements, e.g., with beams, slabs, shells. The theory has to be extended for this case.